ACS NANO

www.acsnano.org

ARTICLE

Gradient Polymer Nanofoams for Encrypted Recording of Chemical Events

Nikolay Borodinov,[†] Anna Paola Soliani,[†] Yuriy Galabura,[†] Bogdan Zdyrko,[†] Carley Tysinger,[†] Spencer Novak,[†] Qingyang Du,[‡] Yizhong Huang,[‡] Vivek Singh,[‡] Zhaohong Han,[‡] Juejun Hu,[‡] Lionel Kimerling,[‡] Anuradha Murthy Agarwal,[‡] Kathleen Richardson,[†,§] and Igor Luzinov*[,†]

[†]Department of Materials Science and Engineering, Clemson University, Clemson, South Carolina 29634, United States

[‡]Microphotonics Center and Department of Materials Science and Engineering, Massachusetts Institute of Technology, Cambridge, Massachusetts 02139, United States

[§]College of Optics and Photonics, University of Central Florida, Orlando, Florida 32816, United States

Supporting Information

ABSTRACT: We have fabricated gradient-grafted nanofoam films that are able to record the presence of volatile chemical compounds in an offline regime. In essence, the nanofoam film (100−300 nm thick) is anchored to a surface cross-linked polymer network in a metastable extended configuration that can relax back to a certain degree upon exposure to a chemical vapor. The level of the chain relaxation is associated with thermodynamic affinity between the polymer chains and the volatile compounds. In our design, the chemical composition of the nanofoam film is not uniform; therefore, the film possesses a gradually changing local affinity to a vapor along the surface. Upon vapor exposure, the nonuniform changes in local film morphology provide a permanent record or "fingerprint" for the chemical event of interest. This permanent modification in the film structure can be directly detected *via* changes not only in the film surface profile but also in the film optical characteristics. To this end, we demonstrated that sensing/recording nanofoam films can be prepared and interrogated on the surfaces of optical waveguides, microring optical resonators. It is important that the initial surface profile and structure of the nanofoam film are encrypted by the distinctive conditions that were used to fabricate the film and practically impossible to replicate without prior knowledge.

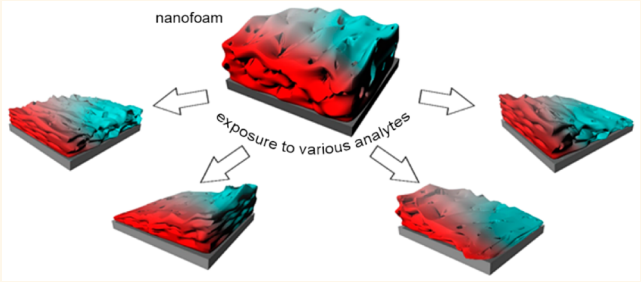

KEYWORDS: *nanofoams, gradient polymer films, polymer grafting, sensors, microring optical resonators*

Sensors for detection of chemicals in the environment have important and irreplaceable applications in law enforcement,[1,2] manufacturing,[3] and homeland security.[4,5] One critical element of a number of sensors developed so far is the nano/microscale polymer-based films deposited onto the sensor measuring elements. The sensing films or their arrays are typically needed to reach the required level of detection by selectively attracting analytes to the sensing element *via* physical/chemical interactions. The vast majority of sensor devices, and, therefore, sensing films, are designed to allow online monitoring to give a rapid response in the presence of an analyte. The ability of the polymer films to recover their initial pre-exposure properties is considered to be one of the key features of the devices, while irreversibility is commonly viewed as a drawback.[6,7]

However, there is also a significant demand for systems employed for offline sensing, where the occurrence of a chemical event can be detected and analyzed *post-factum*. In this case, the information can be recorded through the occurrence of a chemical reaction[8−13] or long-lasting physical changes in the structure of the active sensor material.[14,15] For instance, offline sensing systems are essential in situations where chemical events/incidents might occur but no power and/or connectivity are available. These systems are also important when forensic evidence (*e.g.*, environmental monitoring or international treaty verification) is needed. This requires the development of sensors/sensing polymer films that are capable of accumulating essentially an encrypted signal and being readable in a postexposure regime. It is necessary to point out that the current polymer materials being developed for offline sensing are tailored very specifically to identify certain chemical events. Therefore, in order to detect new substances or chemical events, alternative polymer films or film arrays have to

Received: September 7, 2016
Accepted: October 18, 2016
Published: October 18, 2016

DOI: 10.1021/acsnano.6b06044
ACS Nano 2016, 10, 10716−10725

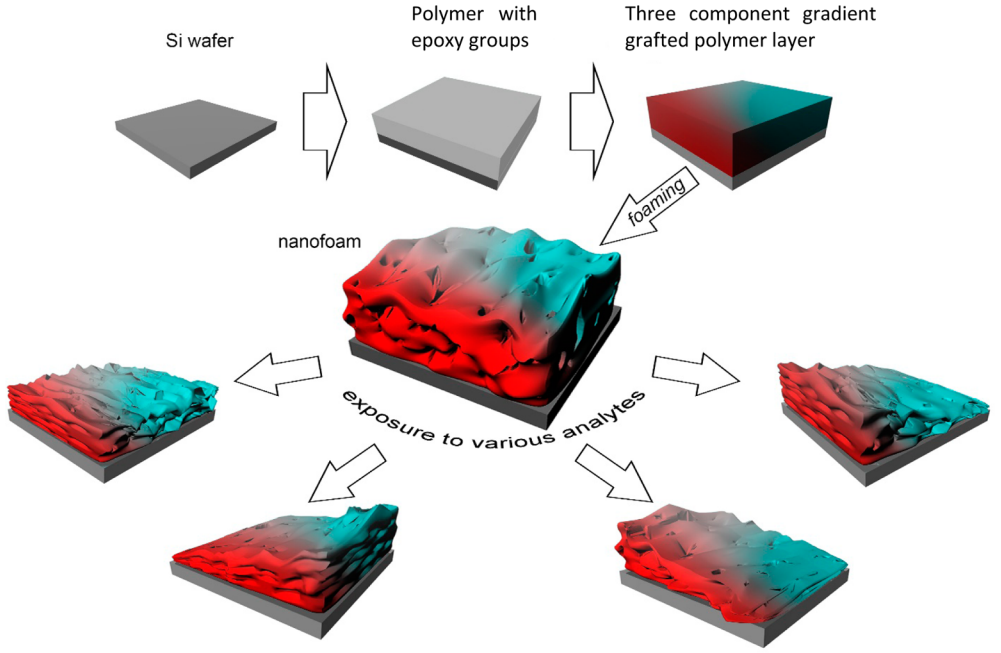

Figure 1. Schematic for the nanofoam film synthesis and operation. Once foamed, the gradient polymer layer can collapse in a solvent-specific way, creating a distinctive permanent pattern.

be developed and tested. To this end, we report here an original and effective approach to the fabrication of polymer films that are able to record the presence of a variety of volatile chemical compounds in an offline regime. The film is made of gradient polymer nanofoam, a tunable sensing material with structurally built-in sensing and recording capabilities.

In general, the nanofoam film is a surface-grafted cross-linked polymer network in a metastable extended configuration that can relax back a certain degree upon exposure to external stimuli. Recently, we reported on a uniform (without a chemical composition gradient) fabrication of the nanofoam and its response to temperature variation.[16] Specifically, the grafted nanofoam was shown to possess the behavior of a shape-memory material,[17] exhibiting gradual mechanical contraction at the nanometer scale as the temperature was increased. We also found that by modification of the nanofoam with polymer grafting, an absolute nanoscale mechanical response of the porous polymer film can be tuned.

Since the contraction of the nanofoam is caused by forces associated with conformational changes of stretched macromolecular chains, it became obvious that the relaxation of the chains can be caused similarly by plasticization of the extended grafted polymer chains with the volatile chemical compounds absorbed by the nanofoam.[18] The degree of the chain relaxation is associated with the thermodynamic affinity between the polymer chains and the volatile compounds. Therefore, the key point in the design of the detecting/monitoring platform reported here is the grafted nanofoam that has prescribed chemical gradients and, therefore, also possesses a gradually changing local affinity to volatile substances along the surface. On exposure to specific analytes, the film locally and irreversibly changes its internal structure at the nanolevel. The structural transformation resulting from the exposure causes significant changes in the thickness and density profile of the polymeric film, which in turn affect local optical properties such as refractive index and optical absorption. The changes in local film morphology under exposure are irreversible and provide a permanent record or "fingerprint" for the chemical event of interest. This permanent modification in the film nanostructure can be directly detected *via* changes in the film surface profile and/or the optical characteristics of the light propagating in the waveguide. It is important to highlight that the initial surface profile and structure of the nanofoam film are encrypted by the distinctive conditions that were used to fabricate the nanoporous film and practically impossible to replicate without prior knowledge.

RESULTS AND DISCUSSION

Gradient Nanofoam Film: Principles of Formation and Operation. The fabrication of the gradient nanofoam film is achieved in four major steps (Figure 1). First, a film made of polymer possessing epoxy groups in monomeric units is deposited on a surface. Second, the film is cross-linked *via* a reaction of the epoxy groups to create a coating that is nonsoluble yet is able to swell. Next, the film is grafted with different polymers capable of reacting with the remaining (unreacted) epoxy functionality. The extent of the film reaction with each polymer is dependent on the spatial location within the film. In essence, we generate a gradient film whose chemical composition varies in two directions. In this way every point of the film possesses its own distinctive composition. Finally, the film is submerged in a solvent or solvent mixture so that it swells and is freeze-dried under reduced pressure. Thus, following the removal of the solvent(s) by sublimation, a nanoporous polymer film is obtained.

The resulting film is below the glass transition temperature (T_g) at the temperatures of operation and possesses the behavior of a nanoscale shape-memory material, which exhibits mechanical action under external stimulus (Figure 1). More specifically, the coating (which is *not* in thermodynamic equilibrium in the porous state) is able to "remember" its original nonporous shape determined by the network elasticity. Exposure of the film to a chemical vapor that interacts with the macromolecules in the film causes plasticization of the film. As

DOI: 10.1021/acsnano.6b06044
ACS Nano 2016, 10, 10716−10725

soon as the macromolecules attract a sufficient amount of the target chemical, the T_g of the polymer chains decreases. Therefore, the chains become mobile and the film shrinks. Since the film possesses a graded chemical composition, different locations of the film interact in different ways with the target chemical. Specifically, certain regions of the film that have a higher thermodynamic affinity to a chemical shrink to a higher extent, creating a distinctive thickness pattern for that specific chemical (Figure 1). The resulting changes in local film morphology are irreversible and provide a permanent record or "fingerprint" for the chemical event of interest.

The obtained record is encrypted by the knowledge of (i) distinctive conditions that were used to fabricate the nanoporous film and (ii) level of the film response upon chemical vapor exposure. In fact, the nanofoam film is produced in two principal steps: synthesis of the gradient polymer film, followed by freeze-drying of the film swollen in a solvent (or solvent mixture). Therefore, the initial surface profile and level of response of the film to the presence of chemical vapors are encrypted by an operator *via* (a) film composition at nano/micro/macrolevels controlled during synthesis; (b) solvent composition, which controls the degree of film swelling prior to and during freeze-drying; and (c) freeze-drying conditions, which include pressure and temperature. Indeed, during our preliminary studies we experimentally determined that these are the parameters controlling the nanofoam morphology and behavior. All of these manipulations are practically impossible to replicate without prior knowledge of the procedures.

In general, the concept of encryption presumes the presence of the "message", protected by the "key", which should be known to decipher the "message". In our case, the "message" is the history of the chemical vapor exposure that leaves the distinctive signature of nanofoam collapse. The "key" is the knowledge of the pattern produced as the nanofoam is exposed to a particular chemical vapor. Once the film collapses upon exposure to a chemical vapor, the only way to erase the pattern is *via* heating the film to above T_g or exposing it to a number of solvents to collapse the surrounding region entirely. These manipulations would provide a clear and definite record of tampering with the device.

Synthesis of the Gradient-Grafted Films. To start with, a poly(glycidyl methacrylate) (PGMA) layer was deposited by dip-coating from a solution onto a silicon wafer and annealed at an elevated temperature (130 °C) in a vacuum oven. In essence, the PGMA layer was fabricated as a thin internally cross-linked film, covalently bound to the native silicon oxide (covering the silicon surface) using its epoxy group functionalities.[16,19] The typical thickness of the anchored PGMA layers was on the level of 100−120 nm, as measured by reflectometry (Figure 2a). Epoxy groups of PGMA not involved in the reaction with the surface and cross-linking could be used for the grafting of other polymer chains to modify the chemical composition of the nanoscale film. In fact, the epoxy polymer has been demonstrated to be an effective anchoring layer for grafting polymers to inorganic and polymeric surfaces using the "grafting to" and "grafting from" approaches.[20−26] In this work we used the "grafting to" approach to modify the film structure utilizing the temperature dependence of the grafting kinetics. Specifically, to create the gradient in chemical composition of the polymer film, we induced a gradient in the grafting temperature along the sample.[27−30]

In particular, we created gradients of polystyrene (PS) and poly(2-vinyl)pyridine (P2VP) by grafting from the melt.[31] We

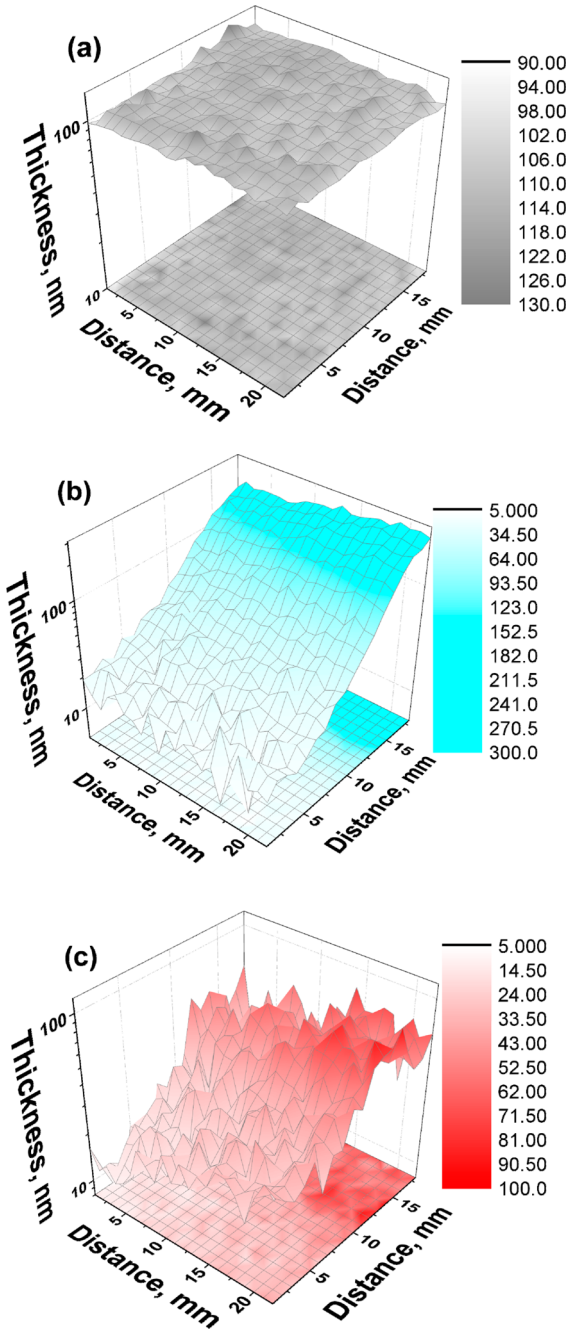

Figure 2. Thickness of the representative grafted layers *versus* surface coordinate: (a) PGMA, (b) PS, (c) P2VP.

selected those polymers to cover a broad range of polymer−environment interactions complementary to PGMA. In fact, the grafted polymer film consisted of hydrogen-bonding/aromatic/basic (P2VP) and hydrophobic/non-hydrogen-bonding/aromatic (PS) polymers. These polymers, as well as PGMA, are in a glassy (low-mobility) state at room temperature.[16,32] The polymers to be grafted possess end-reactive functionality, which was utilized to anchor the polymers to the PGMA layer *via* a reaction between the groups and the functionalities of (carboxyl-terminated) PS and (hydroxyl-terminated) P2VP.[19,25] Since the rate of grafting of the polymers to the PGMA film strongly depends on temperature, we controlled the grafting density by applying a temperature gradient to the sample.[27] First of all, we deposited a carboxy-terminated PS

DOI: 10.1021/acsnano.6b06044
ACS Nano 2016, 10, 10716−10725

layer on the PGMA film by dip-coating and applied a temperature gradient (100−150 °C) to the sample. After removing the unreacted PS from the sample by solvent rinsing, a layer of hydroxyl-terminated P2VP was placed on the surface by dip-coating. For the P2VP anchoring, we applied a temperature gradient (80−130 °C) perpendicular to the temperature gradient used for the attachment of the PS macromolecules. To finalize the formation of the film, any ungrafted P2VP was removed by solvent rinsing. For this study, a total of six parallel gradient samples were prepared.

Figures 2 and 3 display the thickness maps of the fabricated gradient polymer films. The primary PGMA layer is virtually

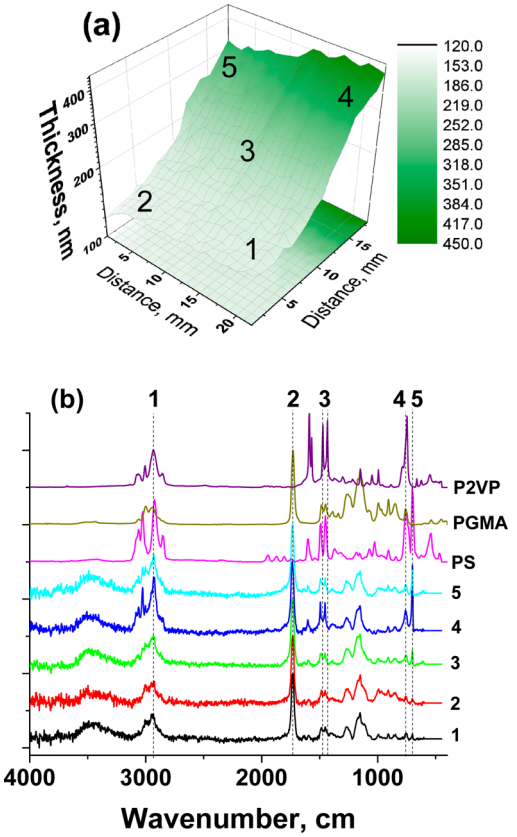

Figure 3. (a) Thickness of the representative three-component gradient-grafted layer *versus* surface coordinate. (b) FTIR spectra of one-component dip-coated films (made of PGMA, PS, and P2VP) and the gradient polymer layer at different locations. The approximate location on the gradient film is marked on (a). The peaks marked are (1) C−H stretching: 2930 cm^{-1}, (2) carbonyl: 1730 cm^{-1}, (3) C−H bending overlapping with aromatic C═C and C═N stretching: 1400−1500 cm^{-1}, (4, 5) C−H bending: 750 and 700 cm^{-1}.

uniform (Figure 2a, Supporting Information (SI) Figure 1S) with an average thickness of 112 nm. The added thickness after the grafting of PS (Figure 2b, SI Figure 1S) ranges from 10 to 270 nm, indicating the successful creation of a PS grafting density gradient. The added thickness after the P2VP attachment (Figure 2c, SI Figures 1S and 2S) varies from 7 to 70 nm. Our results indicate that the P2VP grafting efficiency was dependent not only on the temperature but also on the amount of PS grafted during the previous step. As a result of the temperature/PS grafting density interplay, the grafting procedure resulted in a film with an angle of ∼45° between the PS and P2VP compositional gradients (Figures 2 and 3, SI Figure 2S). A Fourier transform infrared spectroscopy (FTIR) analysis of the resulting gradient film confirmed (Figure 3b, Table S3) that the chemical composition significantly varies across the film. In fact, the ratios between intensities of the major IR absorption peaks, such as C−H stretching (2930 cm^{-1}), carbonyl (1730 cm^{-1}), C−H bending overlapping with aromatic C═C and C═N stretching (1400−1500 cm^{-1}), and C−H bending (750 and 700 cm^{-1}), are distinctive for different locations of the three-component grafted film. There are at least five principal compositional areas that can be virtually identified on the sample (Figure 3, SI Figure 2S) with PGMA/PS/P2VP ratios roughly on the level of (1) 10/1/2, (2) 10/2/1, (3)10/5/3, (4) 10/20/6, and (5) 10/20/4. Atomic force microscopy (AFM) images (Figure 4) clearly show that the areas possess somewhat similar surface morphologies. In general, the AFM root-mean-square (RMS) roughness of the grafted films is on the level of 7−20 nm (SI Figure S4), with a higher roughness in the areas with higher PS and P2VP contents. We suggest that the higher roughness is connected with the mutual immiscibility of the PS, P2VP, and PGMA macromolecules.

Formation of the Nanofoam Film. The foaming consisted of swelling the grafted polymer layer in chloroform followed by freeze−thawing and sublimation of the solvent. Chloroform was selected, as it is a good solvent for all three polymers constituting the film and can be frozen at −59 °C, an experimentally reachable temperature. To swell the polymer film, a small amount of the solvent was placed dropwise on the film surface. Next, the sample was cooled to freeze the chloroform. Finally, the solvent was sublimated under reduced pressure. From visual inspection it was clear that the transparent grafted film became opaque after the solvent sublimation. The loss of transparency indicated a scattering of light because of pore formation. Figure 5 shows the thickness map of the typical fabricated nanofoam gradient polymer films in comparison with a map of the film before the foaming procedure. The thickness of the gradient film (measured by reflectometry) increased in all compositional areas by 17 ± 4%. AFM imaging showed a significant change in morphology of the gradient film after the foaming (Figure 4 and SI Figure S4). Specifically, a formation of pores and a corresponding increase in film roughness were observed. RMS roughness of the film increased from 7−20 nm to 12−27 nm due to the development of the open pores within the layer. To identify whether the grafted nanofoam had pores throughout the film, we conducted an experiment to visualize pore locations in the grafted nanofoam layer. Specifically, a "nanotomography" approach was utilized to analyze the inner structure of the grafted film after solvent sublimation.[16,33] This approach is based on a step-by-step air plasma etching of the film with a subsequent step-by-step AFM analysis of the etched surface, after which the morphology inside the film is revealed. We used low-power air plasma (at 1 min intervals) to etch the film. Reflectometry measurements were used to track the thickness of the etched polymer film after each step. Results of the experiment are presented in the SI (Figures S5 and S6). The AFM imaging revealed that, in fact, pores were situated not only on the surface but also throughout the foamed layer. The sizes of the interconnected and open pores inside the film were estimated to be between 10 and 200 nm.

Operation of the Nanofoam Film as a Sensing/Recording Element. In order to characterize the response

DOI: 10.1021/acsnano.6b06044
ACS Nano 2016, 10, 10716−10725

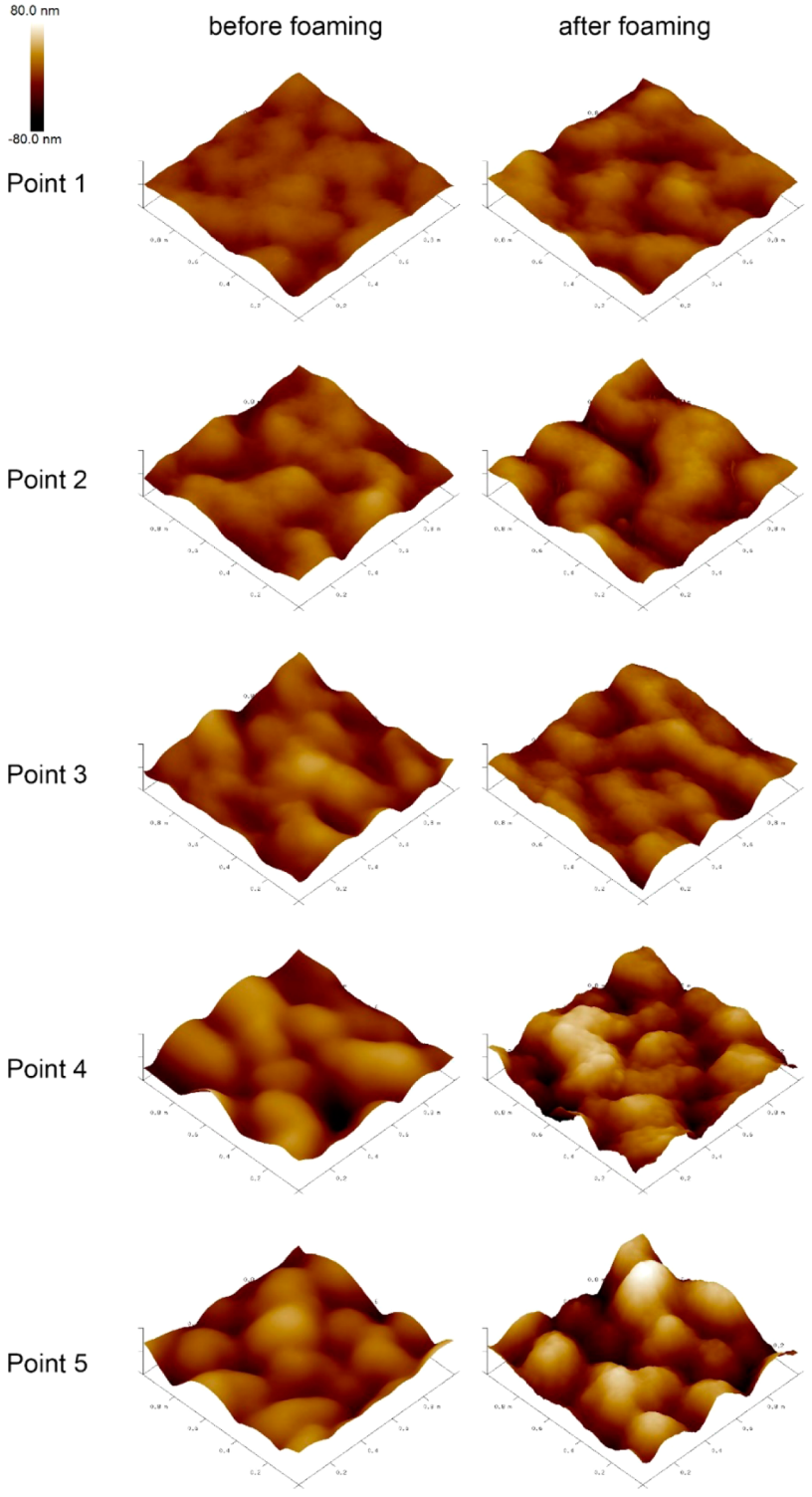

Figure 4. AFM (1 × 1 μm) topographical images for the gradient-grafted layer at different locations before and after the foaming. The approximate location on the gradient film is marked in Figure 3a.

of the gradient nanofoam polymer layer to the vapors of volatile organic compounds, the nanofoam samples were exposed to methanol, toluene, or acetone. The solvents were selected based on their affinity to the macromolecules constituting the gradient nanofoam.[19,27] Acetone was selected, as it is a good solvent for PGMA and a moderate solvent for PS and P2VP. Toluene was chosen, as it is a good solvent for PS, moderate for PGMA, and bad for P2VP. Methanol was selected, as it is a good solvent for P2VP, but bad for the other two components. This set of solvents covers predominantly van der Waals, polar, and hydrogen bonding between a solvent molecule and polymer layer. After the exposure, the samples were evacuated from the solvent vapor and allowed to dry overnight. Next, their thicknesses were mapped using the scanning reflectometer. The extent of collapse at any one point of the sample is defined by a dimensionless parameter alpha:

DOI: 10.1021/acsnano.6b06044
ACS Nano 2016, 10, 10716−10725

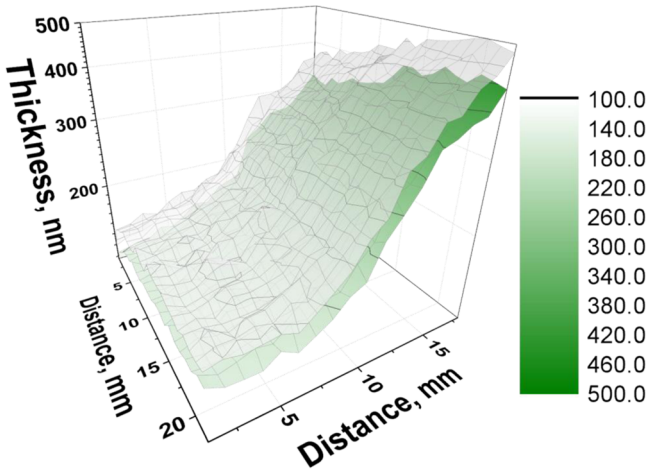

Figure 5. Thickness of the representative gradient-grafted layer *versus* surface coordinate before (bottom) and after (top) the foaming.

$$\alpha = 1 - (d_{\text{exposed}} - d_{\text{initial}})/(d_{\text{foamed}} - d_{\text{initial}})$$

where d_{initial}, d_{foamed}, and d_{exposed} are the initial thickness of the film at the given point, the thickness after foaming, and the thickness after exposure to the solvent vapors, respectively. A higher value of the parameter alpha indicates a higher degree of collapse of the nanofoam. Specifically, the parameter reflects the relative value of the film collapse normalized by the thickness gained during foaming, or it shows the fraction of the added (*via* foaming) thickness that is gone as the result of the vapor exposure. This parameter was selected, as it allows a straightforward comparison of degree of collapse for points on the nanofoam with different absolute thicknesses.

Figure 6 shows the collapse extent (α), equal to 0 for the nonexposed gradient nanofoam (Figure 6a) and the nanofoam exposed to toluene, methanol, and acetone (Figure 6b, c, and d) averaged from three parallel experiments. As it is evident from Figure 6, each solvent generates its own pattern of collapse, which is defined by the interplay between the thermodynamic affinity of the solvent to the polymer layer and the grafting density of PS and P2VP. The observed film collapse is permanent and does not change with time at room temperature. The obtained result clearly demonstrates that the nanofoam gradient polymer film can be used for offline sensing and encrypted recording of chemical events and differentiation between them.

Monitoring of Nanofoam Collapse with Microring Resonators. We also demonstrated that sensing/recording nanofoam films can be prepared and interrogated on the surface of microring optical resonators (Figure 7). Microresonators are extremely sensitive to perturbations in the refractive index of their surroundings as well as any changes in optical absorption.[18,34,35] They offer two different modes of detection that can be exploited for various monitoring

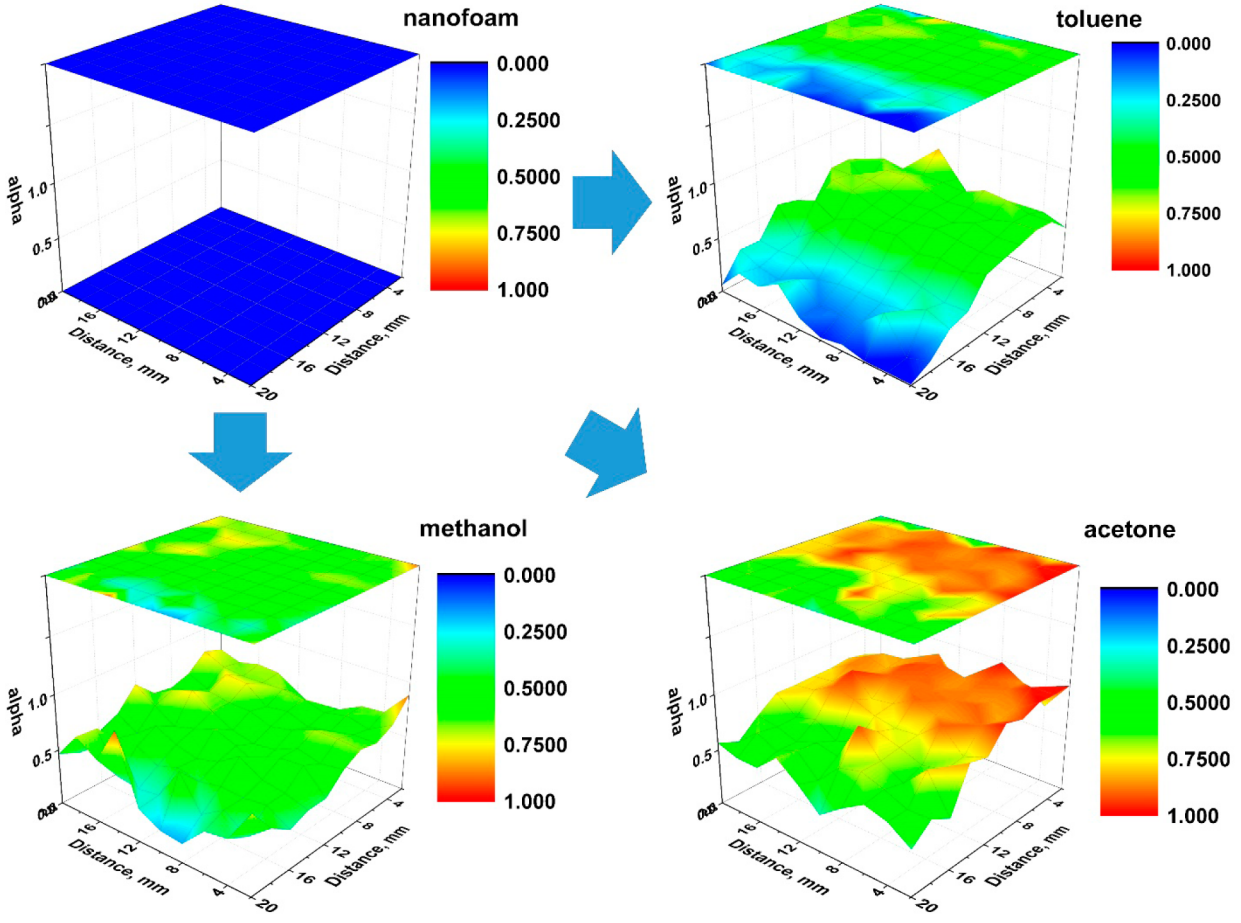

Figure 6. Collapse extent (α) of gradient nanofoam film caused by exposure to vapors of toluene, methanol, and acetone. Three solvents generate drastically different patterns of collapse. The data were averaged for three parallel gradient samples.

DOI: 10.1021/acsnano.6b06044
ACS Nano 2016, 10, 10716–10725

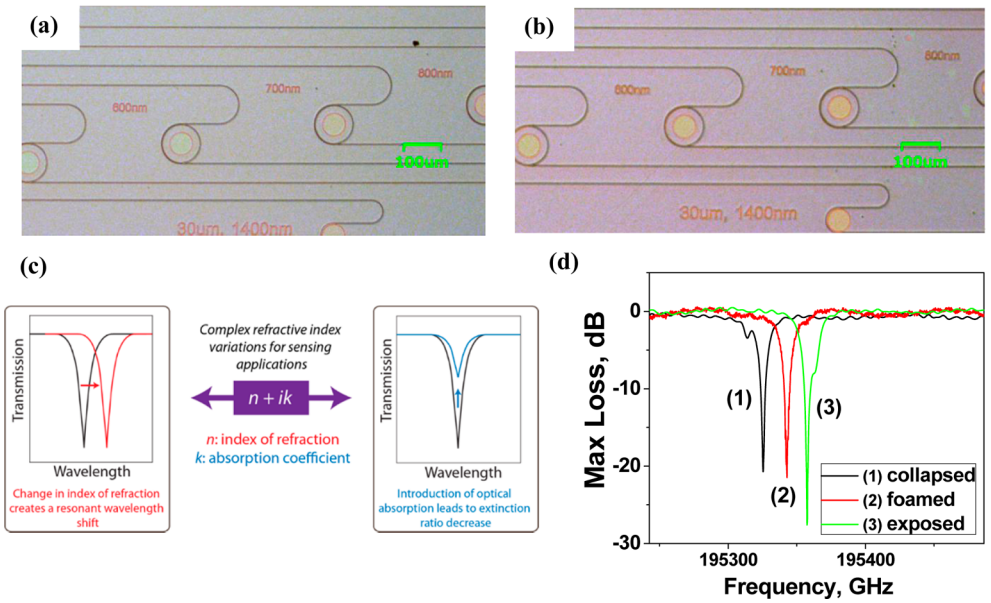

Figure 7. Optical micrographs of the microdisc resonators (a) as fabricated and (b) modified with a PS/PGMA grafted layer. (c) Microresonator resonance peak alteration in the case of changing refractive index (shift) and infrared absorption (peak damping). (d) Example of change in spectrum of the microring resonator covered with nanofoam. The spectra are shown for a PGMA nanofoam before and after exposure to methanol vapor and latter collapsed in liquid chloroform.

applications. As shown in Figure 7c, a change in the refractive index of the surroundings is reflected as a shift in the resonant peak position, while the introduction of optical absorption leads to a change in the peak height or extinction ratio. We previously reported on an effective surface modification of the arrays of optical resonators *via* grafting of nanoscale polymer films for sensing applications.[18,36]

In this work, nanofoam films (single composition, without a gradient) were prepared on the surfaces of optical resonators, and the refractive indices of the films were measured before and after exposure to the solvent vapors. The custom arrays of microring resonators (made of infrared transparent silicon nitride) were fabricated on silicon wafers covered with 3 μm of thermally grown SiO_2. Figure 7a shows a microphotograph of the resonators. The diameter of a microring resonator is 100 μm (0.1 mm). The size of the typical nanofoam film made in this work is on the order of 20 × 20 mm. Therefore, the array, in principle, can allow optical interrogation of the refractive index and optical absorption at different locations on the nanofoam film.

Nanofoam films grafted with PGMA, PS/PGMA, and P2VP/PGMA were fabricated on separate resonator arrays. The thicknesses of the layers (estimated with reflectometry before foaming) were on the level of 80−100 nm for the PGMA layers with an additional ∼90 nm of grafted PS (PS/PGMA layer) and additional ∼50 nm of grafted P2VP (P2VP/PGMA layer). Figure 7b shows that a typical grafted layer quite evenly covers the optical devices. Each larger array with a foamed polymer layer was cleaved into four identical waveguide arrays. The transmission spectrum of each waveguide on the array was acquired before exposure to any solvent to characterize the spectra of the foam coating. Optical testing demonstrated that the devices were not destroyed during the modification (polymer layer deposition and foaming) procedure. Then, the four arrays of microring resonators were exposed to vapors of methanol, acetone, toluene, or chloroform. Vapor contact lasted for 1 h, and then the samples were left in ambient air overnight to allow the solvent to fully evaporate. The resonance peaks were subsequently recorded again and compared with the recordings acquired before the solvent exposure. Also, to obtain the optical characteristics of the collapsed (nonfoamed) grafted layers, the refractive index was measured for the samples that were rinsed in chloroform and then dried. The data obtained were averaged for the waveguides of the same array, as it was found that the coupling gap had no systematic effect on the peak shift. A typical result of our measurements is presented in Figure 7d. It is evident that the refractive index changes significantly when the grafted layer is foamed and exposed to a solvent.

Figure 8 summarizes the results of our measurements for the different nanofoam/solvent vapor combinations. In fact, we found that the volatile organic compounds generate a solvent-specific refractive index change that varies with the chemical composition of the nanofoam film. As evident from the comparison between the solvent responses, it is possible to generate distinctive solvent signatures using three channels of information: PGMA, PS/PGMA, and P2VP/PGMA-coated

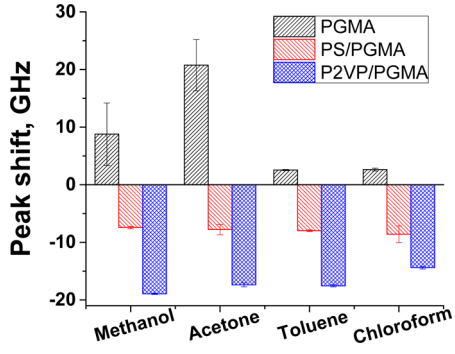

Figure 8. Results of optical transmission measurements for the microring resonators covered with three different nanofoams exposed to four different solvent vapors.

DOI: 10.1021/acsnano.6b06044
ACS Nano 2016, 10, 10716−10725

resonator response. This is a direct demonstration of the ability of microring resonator arrays covered with nanofoams to record the presence of chemicals for further detection in a postexposure regime. It was also found that the most sensitive to the exposure of the solvents (used in this work) are microring resonators covered with PGMA and P2VP/PGMA nanofoams. On the other hand, the resonators covered with PS/PGMA nanofoam show a lower level of optical response. Since the collapse of the nanofoam is dependent on the film composition and grafting density (Figure 6), we foresee that by adjusting those parameters the optical response of the resonators can be tuned to obtain higher sensitivity to exposure to a particular chemical vapor of interest.

CONCLUSION

In conclusion, we have demonstrated that the gradient-grafted nanofoam films are able to record the presence of volatile chemical compounds in an offline regime. Namely, exposure of the nanofoam polymer layer to the solvent vapors causes a controllable collapse of the porous structure that is found to be dependent on the chemical nature of the nanofoam. The collapse is irreversible and solvent-specific, allowing for the use of the nanofoams in the recording of chemical events. The sensing/recording nanofoam films can be prepared and interrogated on the surface of microring optical resonators. It was determined that exposure of the microring resonators covered with the nanofoam films to solvent vapors generates a solvent-specific refractive index change that varies with the chemical composition of the nanofoam film.

MATERIALS AND METHODS

Materials. Glycidyl methacrylate (97%), azoisobutyronitrile (AIBN), poly(ethylene glycol) dimethyl ether (PEG) with number-average molecular weight M_n = 1000 g/mol, sulfuric acid, and hydrogen peroxide (30%) were purchased from Sigma-Aldrich. Monocarboxyl-terminated PS with M_n = 2000 g/mol and hydroxyl-terminated P2VP with M_n = 4000 g/mol were purchased from Polymer Source Inc. Higher molecular weight nonreactive PS (M_n = 170 000 g/mol) was purchased from Sigma-Aldrich. One-sided polished silicon wafers with a thickness of 500 μm were purchased from University Wafer. All solvents used in this work were purchased from VWR International and used as received.

Synthesis of PGMA. PGMA was synthesized according to a previously published procedure.[23] The average molecular weight of the polymer used had M_n = 510 000 g/mol and a polydispersity index (PDI) of 2.2 measured in chloroform *via* gel-permeation chromatography (Waters Breeze) using polystyrene standards.

Formation of Three-Component Gradient Films. The PGMA layer was deposited and anchored according to a previously published procedure.[16] In brief, highly polished, single-crystal, silicon wafers were used as a substrate. The wafers were first cleaned in an ultrasonic bath for 30 min, placed in a hot "piranha" solution (3:1 concentrated sulfuric acid/30% hydrogen peroxide) for 1 h, and then rinsed several times with high-purity water. After rinsing, the substrates were dried under a stream of dry nitrogen. A PGMA layer was deposited on the surface of the wafers by dip-coating (Mayer Feintechnik dip coater, model D-3400) from a 1.5 wt % solution in chloroform. After evaporation of the solvent, the samples were placed in a vacuum oven at an elevated temperature (130 °C) overnight to facilitate the surface attachment and cross-linking of the PGMA macromolecular layer. The layer was then rinsed with the solvent (three to four times) to remove unattached macromolecules. The typical lateral dimensions of the prepared films were on the order of 20 × 20 mm.

To obtain a PS gradient-grafted layer, PGMA-coated Si wafers were dip-coated in a chloroform solution containing 1.2% monocarboxy-PS and 0.3% nonreactive high molecular weight PS. The high molecular weight PS was added to avoid dewetting of the PS film during the annealing. After evaporation of the solvent, the samples were placed on the temperature-gradient stage[37] with the temperature varying from 100 to 150 °C. After 6 h, the PS grafting samples were removed from the stage and thoroughly washed with chloroform (three to four times) to remove any ungrafted PS.

In order to achieve a gradient-grafted layer of P2VP, the samples (already grafted with PS gradient) were dip-coated in a chloroform solution containing 1.5% monohydroxy-P2VP and 1.5% PEG. PEG was used as nonvolatile diluent to increase the level of P2VP penetration into the PS/PGMA film during the grafting. After evaporation of the solvent, the sample was annealed on the gradient stage turned 90° from the position used for the PS grafting. The temperature on the temperature-gradient stage varied from 80 to 130 °C. A total of six parallel samples with a PS/P2VP composition gradient were synthesized and tested in this study.

AFM Imaging. AFM studies were performed on a Dimension 3100 (Digital Instruments) microscope. We used the tapping mode to image the surface morphology of the grafted films. Silicon tips with spring constants of 50 N/m were used. Imaging was done at scan rates in the range of 1−2 Hz. The RMS roughness of our samples was evaluated from the AFM images recorded. Air plasma etching was done using a Harrick PDC-32G plasma cleaner.

FTIR Analysis of 2D Three-Component Orthogonal Gradient Films. The FTIR spectra of the polymer nanoscale layers were acquired using a Thermo Nicolet 6700 FTIR spectrometer equipped with a transmission accessory. A clean Si wafer from the same batch was used as a baseline for the transmission measurements. A total of 256 scans were averaged for each of the five points across the sample.

Measurement of the Film Thicknesses. Spectroscopic reflectometry was performed with a home-built reflectometer (based on the EDMUND Industrial optic spectrometer) at an angle of incidence of 0°. Wavelengths ranging from 400 to 1000 nm were used. The thicknesses and refractive indices of the films were calculated by fitting experimental reflectance using Fresnel equations.[38] The reflectometer has a 2D scanning feature. Specifically, it consists of two T-Cube DC Servo motor controllers connected to a computer *via* a USB and controlled by a LabView graphical user interface, two Thorlabs Z825B motors, two Thorlabs 25 mm motorized translation stages, a waveguide, a BWTEK BRC115P-V-ST1 Exemplar spectrometer, which is also connected to the computer *via* a USB and controlled by the LabView graphical user interface, and a light source. A Si wafer was used for calibration of the optical system at the beginning of the measurement. Fitting of the reflectivity data used an empirical Sellmeier refractive index model[39] with two parameters. Thickness and light source overall intensity drift correction are two other variables, so the total fitting process estimates best fit based on four parameters. A total of 440 points on a 20 × 20 mm scan with 1 mm resolution were measured with a 20 ms acquisition time per point. The foamed films were measured at 2 mm resolution on a 10 × 11 scan four times, and the resulting thicknesses were averaged using Dixon's Q-criteria (90% confidence) to exclude outliers.

Foaming of the PGMA-Based Polymer Thin Films. The foaming was conducted inside a foaming stage,[37] which consists of a vacuum chamber where swelling and solvent sublimation takes place, and a copper temperature-regulated table that was cooled with liquid nitrogen. The table was equipped with a thermocouple that was used to control the temperature of the sample. The gradient films were swollen in a solvent good for all polymers (chloroform) and placed on the temperature-regulated sample table to freeze in their swollen state. The foaming stage was kept at −90 °C using liquid nitrogen, with the subsequent solvent removal (sublimation) done under reduced pressure (50 mmTorr).

Solvent Exposure of the Gradient Nanofoam Films. The samples were exposed to saturated vapors of one of three solvents, toluene, methanol, or acetone, for 40 min. The film thickness profiles were measured and then the samples were refoamed. A total of three exposures were done for each solvent.

Preparation of Silicon Nitride Microresonators. Fabrication of the SiN_x resonators followed the standard Si microfabrication

DOI: 10.1021/acsnano.6b06044
ACS Nano 2016, 10, 10716−10725

processes.[18] Thin-film nitride was grown onto silicon wafers with 3 μm thermal oxide using LPCVD. Photolithography was performed on an i-line stepper to define the resonator patterns in the SiN_x. Subsequently, the patterns were transferred to the film by a reactive ion etch using a mixture of CF_4 and CHF_3 gases. The fabricated silicon nitride waveguide has dimensions of 800 nm (width) by 400 nm (height), and the radius of the resonator is 50 μm.

Polymer Coating of the Silicon Nitride Photonic Resonators. The PGMA layer was deposited on the surface of all three resonator arrays used in this study by dip-coating. PS and P2VP were grafted to the PGMA layers on the surface of respective resonators following the procedure analogous to the one used for the gradient preparation. To reach a high level of grafting, the PS was grafted at 150 °C and the P2VP was grafted at 120 °C. Each layer was subsequently foamed and cleaved into four individual arrays of waveguides so that each array could be exposed to the corresponding solvent.

Optical Transmission Measurement. All transmission measurements were performed on a Newport waveguide measurement system with a tunable laser (1525−1610 nm) coupled to the input facet and a LUNA optical vector analyzer (OVA) coupled to the output facet of the devices with low-loss, lens-tip optical fibers. The optical transmission spectrum was characterized on a Newport Auto Align workstation and an optical vector analyzer (LUNA Technologies OVA-5000) with a built-in tunable laser. Near-infrared wavelength light was coupled in and out through the bus waveguide using a tapered lens-tip fiber. All measurements were performed at a constant temperature of 19.7 ± 0.2 °C. The resonator samples were placed on a static stage, while the input and output fibers were on precise software-controlled, motorized three-axis stages that allow movements as small as 10 nm. The input fiber was aligned by observing the waveguide mode exiting the output facet using an infrared camera. The output fiber was then aligned using an optical power meter to read the power being coupled out of the output facet. The resulting pre-exposure and postexposure spectra for each waveguide were plotted together. A Lorentz peak function was used for the fitting of the corresponding peaks using Origin 2016 software. The peak shift was calculated as the difference between the Lorentz fit centers of the nanofoam spectra before and after exposure. The peak shift values for waveguides of the same array were averaged.

ASSOCIATED CONTENT

Supporting Information

The Supporting Information is available free of charge on the ACS Publications website at DOI: 10.1021/acsnano.6b06044.

Thickness profiles indicating the variation of polymer composition for the three-component grafted gradient film; areas of FTIR peaks presented in Figure 3; AFM RMS roughness for the images presented in Figure 4; AFM images of the nanofoam gradient film before and in the course of the plasma etching (PDF)

AUTHOR INFORMATION

Corresponding Author

*E-mail: luzinov@clemson.edu.

Notes

The authors declare no competing financial interest.

ACKNOWLEDGMENTS

Funding for this work was provided by the Defense Threat Reduction Agency (projects HDTRA1-10-1-0101 and HDTRA1-13-1-0001). The research work of C.T. (undergraduate in the Department of Chemistry, Catawba College, NC, USA) done at Clemson University was supported by National Science Foundation's REU program under grant number DMR REU 1062873. The authors thank M. Savchak (Clemson University) for the preparation of the image used in Figure 1.

REFERENCES

(1) Wren, S. P.; Nguyen, T. H.; Gascoine, P.; Lacey, R.; Sun, T.; Grattan, K. T. V. Preparation of Novel Optical Fibre-Based Cocaine Sensors Using a Molecular Imprinted Polymer Approach. *Sens. Actuators, B* **2014**, *193*, 35−41.

(2) Winther-Jensen, O.; Kerr, R.; Winther-Jensen, B. Alcohol Vapour Detection at the Three Phase Interface Using Enzyme-Conducting Polymer Composites. *Biosens. Bioelectron.* **2014**, *52*, 143−146.

(3) Luzinova, Y.; Zdyrko, B.; Luzinov, I.; Mizaikoff, B. Detecting Trace Amounts of Water in Hydrocarbon Matrices with Infrared Fiberoptic Evanescent Field Sensors. *Analyst* **2012**, *137*, 333−341.

(4) Mizaikoff, B. Waveguide-Enhanced Mid-Infrared Chem/Bio Sensors. *Chem. Soc. Rev.* **2013**, *42*, 8683−8699.

(5) Mlsna, T. E.; Cemalovic, S.; Warburton, M.; Hobson, S. T.; Mlsna, D. A.; Patel, S. V. Chemicapacitive Microsensors for Chemical Warfare Agent and Toxic Industrial Chemical Detection. *Sens. Actuators, B* **2006**, *116*, 192−201.

(6) Wang, D.-H.; Cui, Y.-Z.; Tao, F.-R.; Niu, Q.-F.; Li, T.-D.; Xu, H. A Novel Film of Conjugated Polymer Grafted onto Gelatin for Detecting Nitroaromatics Vapor with Excellent Inhibiting Photobleaching. *Sens. Actuators, B* **2016**, *225*, 319−326.

(7) Potyrailo, R. A.; Surman, C.; Nagraj, N.; Burns, A. Materials and Transducers Toward Selective Wireless Gas Sensing. *Chem. Rev.* **2011**, *111*, 7315−7354.

(8) Chan, C.-Y.; Guo, J.; Sun, C.; Tsang, M.-K.; Tian, F.; Hao, J.; Chen, S.; Yang, M. A Reduced Graphene Oxide-Au Based Electrochemical Biosensor for Ultrasensitive Detection of Enzymatic Activity of Botulinum Neurotoxin A. *Sens. Actuators, B* **2015**, *220*, 131−137.

(9) Zhang, Y.; Zhao, H.; Wu, Z.; Xue, Y.; Zhang, X.; He, Y.; Li, X.; Yuan, Z. A Novel Graphene-DNA Biosensor for Selective Detection of Mercury Ions. *Biosens. Bioelectron.* **2013**, *48*, 180−187.

(10) Vaille, J. R.; Ravotti, F.; Garcia, P.; Glaser, M.; Matias, S.; Idri, K.; Boch, J.; Lorfevre, E.; McNulty, P. J.; Saigne, E.; Dusseau, L. Online Dosimetry Based on Optically Stimulated Luminescence Materials. *IEEE Trans. Nucl. Sci.* **2005**, *52*, 2578−2582.

(11) Angelini, E.; Grassini, S.; Neri, A.; Parvis, M.; Perrone, G. Ieee, Plastic Optic Fiber Sensor for Cumulative Measurements. In *I2mtc: 2009 IEEE Instrumentation & Measurement Technology Conference*, Vols *1*−*3*, 2009; pp 1619−162310.1109/IMTC.2009.5168723.

(12) Rakow, N. A.; Suslick, K. S. A Colorimetric Sensor Array for Odour Visualization. *Nature* **2000**, *406*, 710−713.

(13) McQuade, D. T.; Pullen, A. E.; Swager, T. M. Conjugated Polymer-Based Chemical Sensors. *Chem. Rev.* **2000**, *100*, 2537−2574.

(14) Zhang, Y.; Qiu, J.; Hu, R.; Li, P.; Gao, L.; Heng, L.; Tang, B. Z.; Jiang, L. A Visual and Organic Vapor Sensitive Photonic Crystal Sensor Consisting of Polymer-Infiltrated SiO_2 Inverse Opal. *Phys. Chem. Chem. Phys.* **2015**, *17*, 9651−9658.

(15) You, B.; Ho, C.-H.; Zheng, W.-J.; Lu, J.-Y. Terahertz Volatile Gas Sensing by Using Polymer Microporous Membranes. *Opt. Express* **2015**, *23*, 2048−2057.

(16) Galabura, Y.; Soliani, A. P.; Giammarco, J.; Zdyrko, B.; Luzinov, I. Temperature Controlled Shape Change of Grafted Nanofoams. *Soft Matter* **2014**, *10*, 2567−2573.

(17) Xie, T.; Page, K. A.; Eastman, S. A. Strain-Based Temperature Memory Effect for Nafion and Its Molecular Origins. *Adv. Funct. Mater.* **2011**, *21*, 2057−2066.

(18) Singh, V.; Lin, P. T.; Patel, N.; Lin, H.; Li, L.; Zou, Y.; Deng, F.; Ni, C.; Hu, J.; Giammarco, J.; Soliani, A. P.; Zdyrko, B.; Luzinov, I.; Novak, S.; Novak, J.; Wachtel, P.; Danto, S.; Musgraves, J. D.; Richardson, K.; Kimerling, L. C.; Agarwal, A. M. Mid-Infrared Materials and Devices on a Si Platform for Optical Sensing. *Sci. Technol. Adv. Mater.* **2014**, *15*, 014603.

(19) Bliznyuk, V.; Galabura, Y.; Burtovyy, R.; Karagani, P.; Lavrik, N.; Luzinov, I. Electrical Conductivity of Insulating Polymer Nanoscale Layers: Environmental Effects. *Phys. Chem. Chem. Phys.* **2014**, *16*, 1977−1986.

DOI: 10.1021/acsnano.6b06044
ACS Nano 2016, 10, 10716−10725

(20) Hoy, O.; Zdyrko, B.; Lupitskyy, R.; Sheparovych, R.; Aulich, D.; Wang, J. F.; Bittrich, E.; Eichhorn, K. J.; Uhlmann, P.; Hinrichs, K.; Muller, M.; Stamm, M.; Minko, S.; Luzinov, I. Synthetic Hydrophilic Materials with Tunable Strength and a Range of Hydrophobic Interactions. *Adv. Funct. Mater.* **2010**, *20*, 2240−2247.
(21) Liu, Y.; Klep, V.; Zdyrko, B.; Luzinov, I. Synthesis of High-Density Grafted Polymer Layers with Thickness and Grafting Density Gradients. *Langmuir* **2005**, *21*, 11806−11813.
(22) Ramaratnam, K.; Tsyalkovsky, V.; Klep, V.; Luzinov, I. Ultrahydrophobic Textile Surface *via* Decorating Fibers with Monolayer of Reactive Nanoparticles and Non-Fluorinated Polymer. *Chem. Commun.* **2007**, 4510−4512.
(23) Tsyalkovsky, V.; Klep, V.; Ramaratnam, K.; Lupitskyy, R.; Minko, S.; Luzinov, I. Fluorescent Reactive Core-Shell Composite Nanoparticles with a High Surface Concentration of Epoxy Functionalities. *Chem. Mater.* **2008**, *20*, 317−325.
(24) Samadi, A.; Husson, S. M.; Liu, Y.; Luzinov, I.; Kilbey, S. M. Low-Temperature Growth of Thick Polystyrene Brushes *via* ATRP. *Macromol. Rapid Commun.* **2005**, *26*, 1829−1834.
(25) Zdyrko, B.; Luzinov, I. Polymer Brushes by the ″Grafting to″ Method. *Macromol. Rapid Commun.* **2011**, *32*, 859−869.
(26) Zdyrko, B.; Klep, V.; Li, X. W.; Kang, Q.; Minko, S.; Wen, X. J.; Luzinov, I. Polymer Brushes as Active Nanolayers for Tunable Bacteria Adhesion. *Mater. Sci. Eng., C* **2009**, *29*, 680−684.
(27) Ionov, L.; Sidorenko, A.; Stamm, M.; Minko, S.; Zdyrko, B.; Klep, V.; Luzinov, I. Gradient Mixed Brushes: ″Grafting to″ Approach. *Macromolecules* **2004**, *37*, 7421−7423.
(28) Ionov, L.; Zdyrko, B.; Sidorenko, A.; Minko, S.; Klep, V.; Luzinov, I.; Stamm, M. Gradient Polymer Layers by ″Grafting to″ Approach. *Macromol. Rapid Commun.* **2004**, *25*, 360−365.
(29) Luzinov, I.; Minko, S. Polymer Gradients: Responsive Grafted Layers. In *Soft Matter Gradient Surfaces: Methods and Applications*; Genzer, J., Ed.; Wiley-Blackwell: Hoboken, NJ, 2012.
(30) Luzinov, I.; Minko, S.; Tsukruk, V. V. Responsive Brush Layers: from Tailored Gradients to Reversibly Assembled Nanoparticles. *Soft Matter* **2008**, *4*, 714−725.
(31) Zdyrko, B.; Iyer, K. S.; Luzinov, I. Macromolecular Anchoring Layers for Polymer Grafting: Comparative Study. *Polymer* **2006**, *47*, 272−279.
(32) Bicerano, J. *Prediction of Polymer Properties*, 3rd ed.; Marcel Dekker: New York, NY, 2002.
(33) Usov, D.; Gruzdev, V.; Nitschke, M.; Stamm, M.; Hoy, O.; Luzinov, I.; Tokarev, I.; Minko, S. Three-Dimensional Analysis of Switching Mechanism of Mixed Polymer Brushes. *Macromolecules* **2007**, *40*, 8774−8783.
(34) Hu, J. J.; Sun, X. C.; Agarwal, A.; Kimerling, L. C. Design Guidelines for Optical Resonator Biochemical Sensors. *J. Opt. Soc. Am. B* **2009**, *26*, 1032−1041.
(35) Petit, L.; Carlie, N.; Zdyrko, B.; Luzinov, I.; Richardson, K.; Hu, J. J.; Agarwal, A.; Kimerling, L.; Anderson, T.; Richardson, M. Development of Novel Integrated Bio/Chemical Sensor Systems Using Chalcogenide Glass Materials. *Int. J. Nanotechnol.* **2009**, *6*, 799−815.
(36) Giammarco, J.; Zdyrko, B.; Petit, L.; Musgraves, J. D.; Hu, J.; Agarwal, A.; Kimerling, L.; Richardson, K.; Luzinov, I. Towards Universal Enrichment Nanocoating for IR-ATR Waveguides. *Chem. Commun.* **2011**, *47*, 9104−9106.
(37) Soliani, A. P. *Synthesis and Characterization of Chemically Functionalized Shape Memory Nanofoams for Unattended Sensing Applications*. Ph.D. thesis, Clemson University, 2014.
(38) Siqueiros, J. M.; Regalado, L. E.; Machorro, R. Determination of (n,k) for Absorbing Thin-Films Using Reflectance Measurements. *Appl. Opt.* **1988**, *27*, 4260−4264.
(39) Yovcheva, T.; Vlaeva, I.; Bodurov, I.; Dragostinova, V.; Sainov, S. Refractive Index Investigation of Poly(vinyl alcohol) Films with TiO_2 Nanoparticle Inclusions. *Appl. Opt.* **2012**, *51*, 7771−7775.

DOI: 10.1021/acsnano.6b06044
ACS Nano 2016, 10, 10716−10725